J. Fluid Mech. (2002), *vol.* 454, *pp.* 327–343. © 2002 Cambridge University Press
DOI: 10.1017/S002211200100711X Printed in the United Kingdom

Uniform steady free-surface flow in heterogeneous porous formations

By ORNA AMIR AND GEDEON DAGAN
Department of Fluid Mechanics and Heat Transfer, Faculty of Engineering, Tel Aviv University, Ramat Aviv, Israel

(Received 27 April 2001 and in revised form 14 August 2001)

The effect of spatial variability of the hydraulic conductivity upon free-surface flow is investigated in a stochastic framework. We examine the three-dimensional free-surface gravitational flow problem for a sloped mean uniform flow in a randomly heterogeneous porous medium. The model also describes the interface between two fluids of differing densities, e.g. freshwater/saltwater and water/oil with the denser fluid at rest. We develop analytic solutions for the variance and integral scale of free-surface fluctuations and of specific discharge on the free surface. Additionally, we obtain semi-analytic solutions for the statistical moments of the head and the specific discharge beneath the free surface. Statistical moments are derived using a first-order approximation and then compared with their counterpart in an unbounded medium. The effect of anisotropy and angle of mean uniform flow on the statistical moments is analysed. The solutions can be used for solving more complex flows, slowly varying in the mean.

1. Introduction

Free-surface flows occur in a multitude of hydrological and reservoir engineering applications. Many water bearing formations (aquifers) are unconfined and bounded from above by a water table, which is commonly modelled as a sharp free surface of constant pressure. Likewise, in coastal aquifers freshwater flows above seawater bodies and the separation zone is modelled as a sharp interface. In reservoir engineering a similar configuration occurs for a lighter fluid (oil) flowing above a body of a denser one (water). The drawdown of the water table or the upconing of the interface near pumping wells constitute the main limiting factor of the available discharge. These important applications have motivated a large body of literature on mathematical modelling of free-surface flows in porous media.

The traditional approach is to regard the medium as homogeneous, of constant hydraulic conductivity K. Various approaches to and solutions of free-surface flows have been advanced in the past for such media (e.g. Polubarinova–Kotchina 1962; Bear 1972) and the subject is still a topic of active research in the mathematical and engineering literature.

In the last two decades it was recognized in the hydrological literature that natural formations are heterogeneous and the spatially variable conductivity $K(\boldsymbol{x})$ may change by orders of magnitude in the same geological unit. These variations are of an irregular nature and are characterized by length scales much larger than the pore scale. This intrinsic large-scale heterogeneity may have a large impact on the transport of solutes. The common approach is to model K as a random space function (RSF), characterized by various statistical moments, and to regard the equations of flow as stochastic (e.g. Dagan 1984). Most of the literature deals with the case of mean uniform flows in unbounded domains. A few studies have examined the impact of planar boundaries of given flux (Rubin & Dagan 1988; Lessoff, Indelman & Dagan 2000) or constant pressure head (Rubin, Dagan 1989; Paleologos, Neuman & Tartakovsky 1996).

Very little work has been done, however, on the impact of random heterogeneity upon free-surface flows, which is understandable in view of the problem's complexity. Recently, Dagan & Zeitoun (1998) have derived a few solutions under the Dupuit (shallow water) assumption for a stratified medium, while Fenton & Griffiths (1996), have solved numerically a particular case of two-dimensional flow. Tartakovsky (1999) has derived a complex set of nine integro-differential equations describing the mean and covariance of pressure head and free-surface position under more general conditions, but does not provide analytical or numerical solutions. Most recently, Tartakovsky & Winter (2001) present a more thorough investigation of free-surface flow in a randomly heterogeneous porous medium. Ignoring the effect of gravity on flow in the saturated zone, Tartakovsky & Winter use a first-order asymptotic expansion to obtain governing equations for the covariance of the free-surface position which they then solve analytically in a one-dimensional case.

In the present study we analyse for the first time the impact of heterogeneity of a three-dimensional structure upon free-surface flows. The approach is the aforementioned one: the hydraulic conductivity is regarded as a RSF and so are the dependent variables of interest (pressure head, fluid velocity and free-surface elevation). We aim at determining the statistical moments of these variables. The problem is very complex and there are no exact analytical solutions even for mean uniform flow in unbounded formations, while several have been derived for free-surface flow in homogeneous formations. As a first step toward acquiring a better understanding of the impact of the free surface and for the purpose of comparison with previous approximate solutions for unbounded formations, we address here the simplest case of a mean uniform flow in a semi-infinite domain below a free surface (or above an interface). In a homogeneous medium this problem has an exact solution: a gravity flow of constant velocity, bounded by a sloping, planar, free surface (figure 1). Similarly, a planar interface occurs between a lighter fluid (freshwater) flowing uniformly above a standing denser one (saltwater), with neglect of mixing (figure 1). The spatially variable, random, $K(\boldsymbol{x})$ causes the free surface to fluctuate around its mean position (figure 2) and similarly for other dependent variables. Following the common approach, we assume a stationary and lognormal K, such that $Y = \ln K$ is normal of constant mean m_Y and variance σ_Y^2. To obtain simple, yet illuminating, solutions of an analytical or semi-analytical nature we adopt the same approximation that was used for similar problems in unbounded domains: a first-order approximation in σ_Y. This weak heterogeneity solution has been found to be quite accurate for $\sigma_Y < 1$ for flow in unbounded domains. All flow variables are normal at this order and completely characterized by their mean $O(1)$ and two-point covariances $O(\sigma_Y^2)$.

Zeroth- and first-order terms of the expansion in σ_Y yield the leading-order terms of the mean and mean zero fluctuation, respectively, of flow variables such as hydraulic head, free-surface position and velocity field. In this paper we will begin by describing the mathematical framework of the free-surface flow problem. Using asymptotic expansion, we derive zeroth- and second-order statistical moments of the hydraulic head, the free-surface position, and the velocity field. From these equations we obtain analytic and semi-analytic results which we use to analyse the effect of heterogeneity on flow in the presence of the free surface.

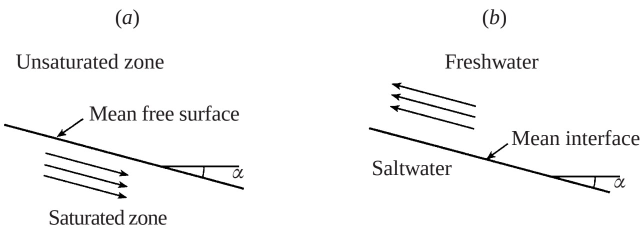

FIGURE 1. (*a*) Free-surface and (*b*) interface flow.

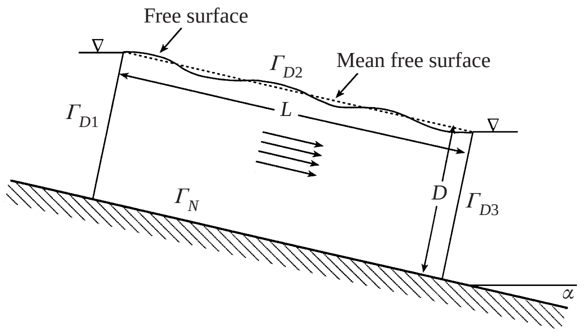

FIGURE 2. Uniform mean flow in a finite domain.

2. Statement of the problem

2.1. *General*

We are interested in modelling flow, which is uniform in the mean, in a heterogeneous medium bounded by a free surface from above. The log of conductivity $Y = \ln(K)$ is taken to be normal as is most frequently the case in field investigations. As such, it is fully described by its mean and two-point covariance. We will consider here for illustration the particular case where the covariance has a Gaussian anisotropic structure, e.g. $C_Y(\boldsymbol{x}, \tilde{\boldsymbol{x}}) = \sigma_Y^2 \exp[-\pi(x-\tilde{x})^2/4I_x^2 - \pi(y-\tilde{y})^2/4I_y^2 - \pi(z-\tilde{z})^2/4I_z^2]$.

Steady-state flow in a saturated porous medium is described by the continuity equation and Darcy's law,

$$\nabla \cdot \boldsymbol{q}(\boldsymbol{x}) = 0, \tag{2.1}$$

$$\boldsymbol{q}(\boldsymbol{x}) = -K(\boldsymbol{x})\nabla\varphi \tag{2.2}$$

respectively, where $\boldsymbol{q}$ is specific discharge, K is hydraulic conductivity, $\varphi = (p/\gamma)+z$ is the head, p is the pressure, γ is the fluid specific weight and z is a vertical coordinate. Combining (2.1) and (2.2) leads to

$$\nabla \cdot [K(\boldsymbol{x})\nabla\varphi] = 0. \tag{2.3}$$

Equation (2.3) is typically solved subject to the following boundary conditions:

$$\varphi(\boldsymbol{x}, t) = \Phi(\boldsymbol{x}) \qquad (\boldsymbol{x} \in \Gamma_D), \tag{2.4}$$

$$q(\boldsymbol{x}, t) \cdot \boldsymbol{n}(\boldsymbol{x}) = Q(\boldsymbol{x}) \quad (\boldsymbol{x} \in \Gamma_N), \tag{2.5}$$

where Γ_D is a Dirichlet boundary, Γ_N is a Neumann boundary, and $\boldsymbol{n}(\boldsymbol{x})$ is a unit vector normal to the boundary.

The boundary condition for uniform flow in an infinite medium is

$$\varphi = -\boldsymbol{J} \cdot \boldsymbol{x} \quad (\boldsymbol{x} \in \Gamma_D). \tag{2.6}$$

when the boundary Γ_D is let to expand to infinity. For instance, this can be seen as the limiting case for the finite domain shown in figure 2, as $D \to \infty$ and $L \to \infty$, where the conditions on the boundaries Γ_{D1} and Γ_{D3} are of constant head, and the condition on the Neumann boundary Γ_N is of no flow, i.e.

$$\varphi(\boldsymbol{x}) = \varphi_A \qquad (\boldsymbol{x} \in \Gamma_{D1}), \tag{2.7}$$

$$\varphi(\boldsymbol{x}) = \varphi_B \qquad (\boldsymbol{x} \in \Gamma_{D3}), \tag{2.8}$$

$$\nabla\varphi(\boldsymbol{x}) \cdot \boldsymbol{n} = 0 \quad (\boldsymbol{x} \in \Gamma_N). \tag{2.9}$$

Equations (2.7)–(2.9) are a particular case of (2.6) with $\boldsymbol{J}$ parallel to the bottom and $|J| = (\varphi_A - \varphi_B)/L$, or equivalently, $|J| = \sin\alpha$.

The solution of this problem is greatly complicated when part of the boundary Γ is made up of a free surface, i.e. a boundary whose shape is unknown *a priori*, rendering this problem nonlinear. Two classic free-surface problems in hydrology and in petroleum engineering are the determination of the interface between the saturated and unsaturated zones (free surface) and between two fluids of differing densities. On the interface between the saturated and unsaturated zones, the free-surface boundary condition is of zero pressure, i.e. $\varphi = z$. Additionally, the free surface is a streamsurface and thus there is no flow normal to it. Hence, the two conditions on the free surface $z = \eta(x, y)$ are

$$\varphi(x, y, z) = z \qquad (z = \eta), \tag{2.10}$$

$$\boldsymbol{q}(x, y, z) \cdot \boldsymbol{n} = 0 \quad (z = \eta). \tag{2.11}$$

By substituting $\boldsymbol{n} \sim (\partial\eta/\partial x, \partial\eta/\partial y, -1)$ and using Darcy's Law (2.2) equation (2.11) becomes

$$\frac{\partial\varphi}{\partial z} - \frac{\partial\eta}{\partial x}\frac{\partial\varphi}{\partial x} - \frac{\partial\eta}{\partial y}\frac{\partial\varphi}{\partial y} = 0 \quad (z = \eta). \tag{2.12}$$

In the case of one fluid uniformly flowing above a denser stationary fluid as in the case with fresh/saltwater and oil/water (figure 1), the interface condition of pressure continuity yields

$$\varphi(x, y, z) = -\frac{\Delta\gamma}{\gamma_1} z \quad (z = \eta), \tag{2.13}$$

where γ_1 is the density of the lighter fluid, $\Delta\gamma = \gamma_2 - \gamma_1$ is the difference in densities of the two fluids, Bear (1972). Since the kinematical condition (2.12) remains unchanged, it is seen that the two problems (2.10), (2.12) and (2.13), (2.12) are equivalent if in the second one we replace φ by $-(\gamma_1/\Delta\gamma)\varphi$. We shall therefore refer only to the free-surface problem in what follows.

2.2. *First-order approximation*

In order to solve for the statistical moments of flow variables in a stationary mildly heterogeneous medium in which the variance of the log conductivity $Y = \ln(K)$ is small, we expand all terms in the governing equation (2.3), and the boundary conditions (2.10), (2.12) in orders of σ_Y. Substituting first $K(\boldsymbol{x}) = \exp[Y(\boldsymbol{x})]$ into (2.3) and assuming that Y is stationary, our governing equation becomes

$$\Delta\varphi + \nabla Y' \cdot \nabla\varphi = 0 \quad (z \leqslant \eta) \tag{2.14}$$

supplemented by the boundary conditions (2.10), (2.12). Here, $Y(\boldsymbol{x}) = m_Y + Y'(\boldsymbol{x})$, where the mean $m_Y = \langle Y \rangle$ is a constant and $Y'(\boldsymbol{x}) = Y - m_Y$ is its fluctuation.

Since we investigate a flow that is uniform in the mean with a sloped mean free surface (figure 1), it is useful to operate in the transformed system $\boldsymbol{x}'$

$$x = x' \cos(\alpha) + z' \sin(\alpha), \tag{2.15}$$

$$z = -x' \sin(\alpha) + z' \cos(\alpha), \tag{2.16}$$

where x', y' are parallel to $\boldsymbol{J}$ and z' is normal. This renders the governing equations (2.14), (2.10), (2.12) of the form

$$\Delta\varphi + \nabla Y' \cdot \nabla\varphi = 0 \quad (z < \eta) \tag{2.17}$$

$$\varphi(x, y, z) = -x \sin\alpha + \eta \cos\alpha \quad (z = \eta), \tag{2.18}$$

$$\frac{\partial\varphi}{\partial z} - \frac{\partial\eta}{\partial x}\frac{\partial\varphi}{\partial x} - \frac{\partial\eta}{\partial y}\frac{\partial\varphi}{\partial y} = 0 \quad (z = \eta). \tag{2.19}$$

where for simplicity we have retained here and in what follows the notation $\boldsymbol{x} = (x, y, z)$ for the sloped system (figure 2). These are the exact equations and the starting point for the perturbation expansion

$$Y = m_Y + Y', \tag{2.20}$$

$$\varphi = \varphi_0 + \varphi_1 + \cdots, \tag{2.21}$$

$$\eta = \eta_0 + \eta_1 + \cdots, \tag{2.22}$$

$$\varphi(x, y, \eta) = \varphi_0(x, y, \eta_0) + \varphi_1(x, y, \eta_0) + \eta_1 \frac{\partial\varphi_0(x, y, \eta_0)}{\partial z} + \cdots, \tag{2.23}$$

where φ_0, η_0 are $O(1)$ and φ_1, η_1 are $O(Y')$.

Substituting the first-order expansions of φ and η into the transformed flow equations (2.17)–(2.19) yields at zero order for the mean head $\varphi_0 = \langle\varphi\rangle + O(\sigma_Y^2)$

$$\Delta\varphi_0 = 0 \qquad (z \leqslant \eta_0), \tag{2.24}$$

$$\nabla\varphi_0 = (-\sin\alpha, 0, 0) \qquad (\boldsymbol{x} \to \infty), \tag{2.25}$$

$$\varphi_0(x, y, \eta_0) = -x \sin(\alpha) + \eta_0 \cos(\alpha) \quad (z = \eta_0(x, y)), \tag{2.26}$$

$$\frac{\partial\varphi_0}{\partial z} - \frac{\partial\eta_0}{\partial x}\frac{\partial\varphi_0}{\partial x} - \frac{\partial\eta_0}{\partial y}\frac{\partial\varphi_0}{\partial y} = 0 \qquad (z = \eta_0(x, y)), \tag{2.27}$$

where α is the slope of the mean gradient $\boldsymbol{J} = (\sin\alpha, 0, 0)$ with respect to the horizontal direction (figure 1). The exact solution to these equations is $\varphi_0 \equiv -x \sin\alpha$, $\eta_0 \equiv 0$, i.e. gravitational free-surface flow in a homogeneous medium (figure 2).

Expanding (2.17)–(2.19) at first order, with $\varphi_0 = -x \sin\alpha$, yields for φ_1

$$\Delta\varphi_1 - \sin\alpha \frac{\partial Y'}{\partial x} = 0 \quad (z \leqslant 0), \tag{2.28}$$

$$\eta_1 = \frac{\varphi_1(x, y, 0)}{\cos\alpha} \qquad (z = 0), \tag{2.29}$$

$$\frac{\partial\varphi_1}{\partial z} + \tan\alpha \frac{\partial\varphi_1}{\partial x} = 0 \quad (z = 0), \tag{2.30}$$

Equations (2.28)–(2.30) for the first-order approximation constitute the starting point for the developments of the rest of the present study. Since $\langle\varphi_1\rangle = 0$ and $\langle\eta_1\rangle = 0$, φ_1 and η_1 are the leading-order terms of the fluctuations of φ and η

respectively. Hence, from this point on we take C_φ and C_η to be given by their second-order approximations, C_{φ_1} and C_{η_1} respectively. Furthermore, due to the linear dependence on Y' in (2.28), both φ_1 and η_1 are normal and characterized completely by their second moments.

The linearization of the exact equations (2.14), (2.10), (2.12) results in three major simplifications: (i) φ_1 satisfies a Poisson equation with a random forcing term, which has been used widely in solving problems in unbounded domains. Here, it applies to the half-space $z \leqslant 0$; (ii) the free-surface boundary condition for φ_1 is linearized and posed on $z = 0$; and (iii) after solving for φ_1, (2.29) renders η_1 in a simple manner. The linearized free-surface boundary conditions do not depend on K and they are the same as the ones employed for solving flow in homgeneous medium under the assumption of small departure of the free surface from a plane (see e.g. Dagan 1989).

The mixed boundary condition on the free surface, (2.30), is the crux of the matter since it includes the slope of the mean free surface. It has two simple asymptotic limits: (i) for $\alpha \ll 1$ it degenerates to a condition of normal zero flux, i.e. a rigid wall at $z = 0$ (this is the case of major interest in hydrological and reservoir engineering applications for which flow is primarily in the horizontal direction), and (ii) $\alpha \to \pi/2$, i.e. the mean free surface is close to vertical, the condition becoming now of zero head fluctuation. This would describe, for instance, a vertical gravitational flow from a ponded soil surface. It is instructive to see that these two extreme cases, a rigid wall and a pressure relief condition, are similar to the ones of small or large Froude numbers for free-surface flow of an ideal liquid. However, the structure of the free-surface condition is different for finite α.

In principle we could first solve (2.28)–(2.30) for φ_1 and η_1 and obtain subsequently the moments of interest of these random variables. It was found to be easier, in terms of mathematical manipulations, to solve directly the equations satisfied by these moments.

3. Statistical moments of the head and the free-surface profile

We derive now the two-point covariances $C_{\varphi Y}(\boldsymbol{x}, \tilde{\boldsymbol{x}}) = \langle \varphi_1(\boldsymbol{x}) Y'(\tilde{\boldsymbol{x}}) \rangle$, $C_\varphi(\boldsymbol{x}, \tilde{\boldsymbol{x}}) = \langle \varphi_1(\boldsymbol{x}) \varphi_1(\tilde{\boldsymbol{x}}) \rangle$ and $C_\eta(\boldsymbol{x}, \tilde{\boldsymbol{x}}) = \langle \eta_1(\boldsymbol{x}) \eta_1(\tilde{\boldsymbol{x}}) \rangle$. These moments are $O(\sigma_Y^2)$ and neglected terms are of $O(\sigma_Y^4)$. Since all the variables are normal, these covariances define completely the joint statistical structure of the Y', φ_1 fields in terms of the given $C_Y(\boldsymbol{x} - \tilde{\boldsymbol{x}})$. For the latter, we shall carry out detailed computations for the particular case of axisymmetric Gaussian $C_Y = \exp[-(\pi r^2)/(4I^2) - \pi(z - \tilde{z})^2/(4I_v^2)]$, where $\boldsymbol{r} = (x - \tilde{x}, y - \tilde{y})$ is a two-dimensional vector in a plane parallel to the mean free surface with $r = |\boldsymbol{r}|$. This is similar to the more general covariance mentioned in § 2.1, except that we assume that the principal axes of anisotropy are now parallel (I) and normal (I_v) to the mean free surface. Keeping the anisotropy axes fixed, while rotating the mean free surface, would have complicated the computations.

We start with the cross-covariance $C_{\varphi Y}$ whose governing equations are obtained by multiplying (2.28)–(2.30) by $Y'(\tilde{\boldsymbol{x}})$ and averaging,

$$\Delta C_{\varphi Y}(\boldsymbol{x}, \tilde{\boldsymbol{x}}) - \sin\alpha \frac{\partial C_Y(\tilde{\boldsymbol{x}}, \boldsymbol{x})}{\partial x} = 0 \qquad (z \leqslant 0), \tag{3.1}$$

$$\frac{\partial C_{\varphi Y}(\boldsymbol{x}, \tilde{\boldsymbol{x}})}{\partial z} + \tan\alpha \frac{\partial C_{\varphi Y}(\boldsymbol{x}, \tilde{\boldsymbol{x}})}{\partial x} = 0 \quad (z = 0), \tag{3.2}$$

where the Laplacian is in terms of $\boldsymbol{x}$.

In a similar manner we multiply (2.28)–(2.30) by $\varphi_1(\tilde{\boldsymbol{x}})$ and average. This yields

$$\Delta C_\varphi(\boldsymbol{x},\tilde{\boldsymbol{x}}) - \sin\alpha \frac{\partial C_{\varphi Y}(\tilde{\boldsymbol{x}},\boldsymbol{x})}{\partial x} = 0 \quad (z \leqslant 0), \tag{3.3}$$

$$\frac{\partial C_\varphi(\boldsymbol{x},\tilde{\boldsymbol{x}})}{\partial z} + \tan\alpha \frac{\partial C_\varphi(\boldsymbol{x},\tilde{\boldsymbol{x}})}{\partial x} = 0 \quad (z = 0). \tag{3.4}$$

Due to the stationarity in the (x, y)-plane, all the aforementioned two-point covariances are functions of the variables $\boldsymbol{r}$, z and $\tilde{z}$ (see Appendix (A 1)–(A 4)).

It is seen that the two covariances satisfy similar equations. Our methodology to solve them is to take the Fourier transform of the two sets of equations in the $\boldsymbol{r}$-plane, reducing the problem to the ODE (ordinary differential equation) in z, shown in Appendix A, (A 5)–(A 8). The analytic solutions for the Fourier transforms of $C_{\varphi Y}$ and C_φ are then given in terms of the Green function $G(z, \xi, \boldsymbol{k})$ as

$$\hat{C}_{\varphi Y}(\boldsymbol{k}, z, \tilde{z}) = -\mathrm{i}k_1 \sin\alpha \int_{-\infty}^{0} G(z, \xi, \boldsymbol{k}) \hat{C}_Y(\boldsymbol{k}, \xi, \tilde{z}) \mathrm{d}\xi, \tag{3.5}$$

$$\hat{C}_\varphi(\boldsymbol{k}, z, \tilde{z}) = -\mathrm{i}k_1 \sin\alpha \int_{-\infty}^{0} G(z, \xi, \boldsymbol{k}) \hat{C}_{\varphi Y}(-\boldsymbol{k}, \tilde{z}, \xi) \mathrm{d}\xi, \tag{3.6}$$

where the Fourier transform is defined as

$$\hat{f}(\boldsymbol{k}) = (1/2\pi) \int_{-\infty}^{\infty} \int_{-\infty}^{\infty} f(r_x, r_y) \exp(\mathrm{i}\boldsymbol{k} \cdot \boldsymbol{r}) \mathrm{d}r_x \mathrm{d}r_y$$

with $\boldsymbol{k} = (k_x, k_y)$ and $\kappa = |\boldsymbol{k}|$. Here, the Green function $G(z, \xi, \boldsymbol{k})$ satisfies the equation

$$(G)_{zz} - \kappa^2 G = \delta(z - \xi) \quad (z \leqslant 0), \tag{3.7}$$

$$(G)_z - \mathrm{i}k_1 \tan\alpha G = 0 \quad (z = 0), \tag{3.8}$$

with solution

$$G(z, \xi, k) = -\frac{\kappa + \mathrm{i}bk_1}{2\kappa(\kappa - \mathrm{i}bk_1)} \mathrm{e}^{\kappa(\xi + z)} - \frac{1}{2\kappa} \begin{cases} \mathrm{e}^{\kappa(\xi - z)}, & z \geqslant \xi, \\ \mathrm{e}^{\kappa(z - \xi)}, & z \leqslant \xi, \end{cases} \tag{3.9}$$

where $b = \tan\alpha$.

Using the Gaussian covariance for Y, $\hat{C}_Y$ is given by

$$\hat{C}_Y(\boldsymbol{k}, z, \tilde{z}) = \frac{2\sigma_Y^2 I^2}{\pi} \exp\left(-\frac{\pi(z - \tilde{z})^2}{4I_v^2} - \frac{\kappa^2 I^2}{\pi}\right). \tag{3.10}$$

Substituting (3.9) and (3.10) into (3.5), we find that $\hat{C}_{Y\varphi}$ and $\hat{C}_\varphi$ can be computed analytically (see Appendix A, (A 9)–(A 10)). For illustration, on the free surface, with $\tilde{z} = z = 0$, $\hat{C}_{Y\varphi}$ and $\hat{C}_\varphi$ simplify to

$$\hat{C}_{\varphi Y}(\boldsymbol{k}, 0, 0) = \frac{2\mathrm{i}\sin\alpha\sigma_Y^2 I^2 I_v}{\pi} \exp\left(-\frac{(I^2 - I_v^2)\kappa^2}{\pi}\right) \left[\frac{k_1(\kappa + \mathrm{i}bk_1)}{(\kappa^2 + b^2 k_1^2)} \mathrm{erfc}\left(\frac{\kappa I_v}{\pi^{1/2}}\right)\right], \tag{3.11}$$

$$\hat{C}_\varphi(\boldsymbol{k}, 0, 0) = \frac{2\sin^2\alpha\sigma_Y^2 I^2 I_v}{\pi} \exp\left(-\frac{(I^2 - I_v^2)\kappa^2}{\pi}\right) \left[\frac{k_1^2}{\kappa(\kappa^2 + b^2 k_1^2)} \mathrm{erfc}\left(\frac{\kappa I_v}{\pi^{1/2}}\right)\right]. \tag{3.12}$$

To grasp the impact of the presence of a free surface on flow, we analyse and discuss a few statistical measures of interest. The variance σ_φ^2, as a function of the

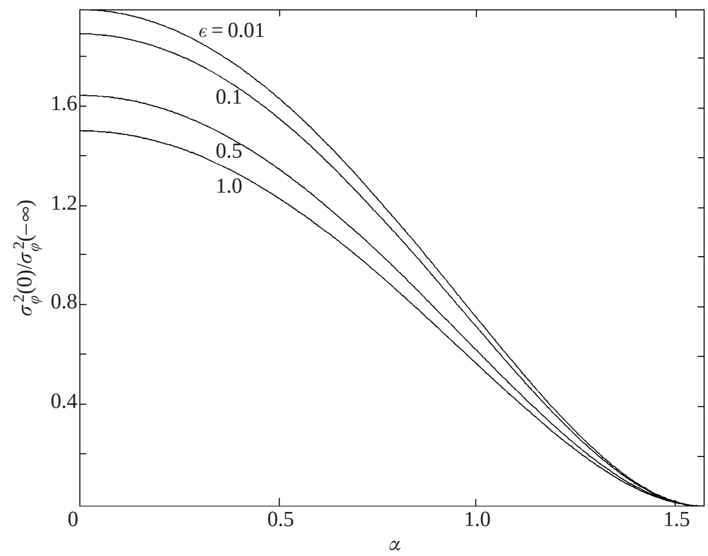

FIGURE 3. Normalized variance of φ_1 on the free surface, $\sigma_\varphi^2(0)/\sigma_\varphi^2(-\infty)$, as a function of α for several values of $\epsilon = I_v/I$, the anisotropy ratio.

distance to the free surface z, is obtained by inverting $\hat{C}_\varphi$ for $\boldsymbol{r} = 0$, $z = \tilde{z}$. For $z = 0$, i.e. on the free surface, the integrations can be completed analytically, yielding

$$\sigma_\varphi^2(0) = \frac{2\cos^2\alpha(1-\cos\alpha)II_v\sigma_Y^2}{\pi(1-\epsilon^2)^{1/2}} \arctan\left(\frac{1-\epsilon^2}{\epsilon^2}\right)^{1/2}, \qquad (3.13)$$

where $\epsilon = I_v/I$ is the anisotropy ratio. For $I_v = I$, this reduces to $\sigma_\varphi^2(0) = 2\cos^2\alpha(1 - \cos\alpha)I^2\sigma_Y^2/\pi$. A similar calculation for the mixed moment of φ and Y, $C_{\varphi Y}(\boldsymbol{r}, z, \tilde{z})$, when $\boldsymbol{r} = 0$ and $z = \tilde{z} = 0$ yields $C_{\varphi Y}(\boldsymbol{0}, 0, 0) = -\cos\alpha(1-\cos\alpha)I_v\sigma_Y^2/(1+\epsilon)$.

The limit of $\sigma_\varphi^2(z)$ as $z \to -\infty$ can also be determined analytically, namely

$$\sigma_\varphi^2(-\infty) = \frac{\sin^2\alpha II_v\sigma_Y^2}{2\pi(1-\epsilon^2)}\left(\epsilon + \frac{1-2\epsilon^2}{(1-\epsilon^2)^{1/2}}\arctan\left(\frac{1-\epsilon^2}{\epsilon^2}\right)^{1/2}\right), \qquad (3.14)$$

which simplifies to $\sigma_\varphi^2(-\infty) = 2\sin^2\alpha I^2\sigma_Y^2/(3\pi)$ in an isotropic medium. This is similar to the expression for σ_φ^2 in an unbounded domain and for an exponential C_Y (Dagan 1989).

To illustrate the results, the normalized variance, $\sigma_\varphi^2(0)/\sigma_\varphi^2(-\infty)$, which depends only on α and the anisotropy ratio $\epsilon = I_v/I$, is represented in figure 3. This ratio reflects the impact of the bounded domain and the free-surface condition on the head fluctuations. Inspection of figure 3 shows that the relative head variance is indeed maximal for $\alpha = 0$, i.e. for flow beneath a rigid wall, and reduces to zero for a vertical mean free-surface position ($\alpha = \pi/2$). This is in agreement with our previous discussion of these limit cases. If $\sigma_\varphi^2(0)$ is made dimensionless with respect to the heterogeneity length scale I^2, the dependence on α has a different nature: it is zero for $\alpha = 0$ (rest) and $\alpha = \pi/2$ (pressure relief) with a maximum at $\alpha = \cos^{-1}(2/3)$. Additionally, we see that the anisotropy increases the variance of head relative to an unbounded domain, no matter what the angle of mean uniform flow.

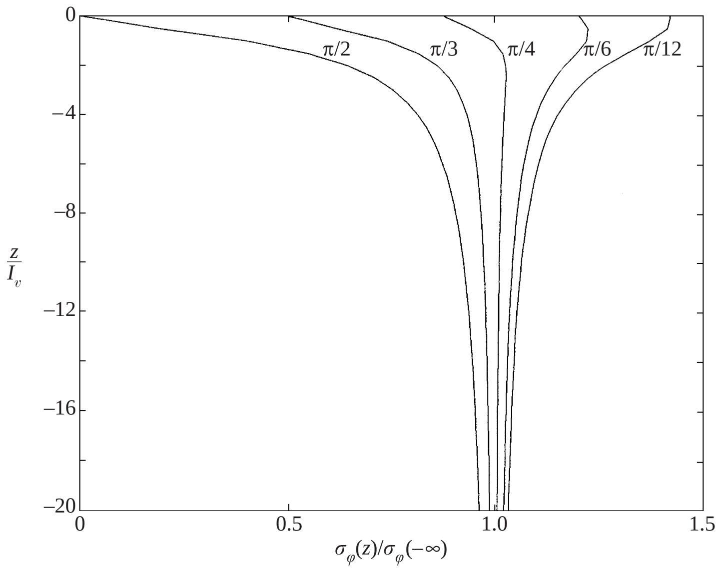

FIGURE 4. Normalized variance of φ_1 as a function of dimensionless depth z/I_v in an isotropic medium for several angles of mean incline, $\alpha = \pi/2, \pi/3, \pi/4, \pi/6, \pi/12$.

Another aspect of the impact of the free surface is revealed by the change of $\sigma_\varphi^2(z)/\sigma_\varphi^2(-\infty)$ with z for fixed α and ε. This was obtained by a numerical quadrature and is represented in figure 4 for several values of α, when $\epsilon = 1$ (isotropic media). The striking result is the slow convergence of $\sigma_\varphi^2(z)$ to $\sigma_\varphi^2(-\infty)$. This can be understood from the inspection of the head variogram in an unbounded domain when α is close to $\pi/2$. It can be seen (Dagan 1989, equation 3.7.12) that the decay of the transverse variogram with distance z is like z^{-1}, i.e. the integral scale is unbounded. Since the boundary condition for $\pi/2$, $\varphi_1 = 0$, is equivalent to conditioning by given φ in an unbounded domain, the impact propagates at large distances.

It is worth emphasizing that the analytical solution for a rigid wall boundary is of interest in itself. In that case we replace $\sin\alpha = J$ in the above results for φ and let $b = \tan\alpha \to 0$ while J is kept fixed.

We analyse next the statistics of the free-surface fluctuations, which is one of the main objectives of this study. As the variance of the free-surface position is directly related to the variance of φ_1 via (2.29), we have

$$\sigma_\eta^2 = \frac{2(1-\cos\alpha)II_v\sigma_Y^2}{\pi(1-\epsilon^2)^{1/2}} \arctan\left(\frac{1-\epsilon^2}{\epsilon^2}\right)^{1/2}, \tag{3.15}$$

which simplifies to $\sigma_\eta^2 = 2(1-\cos\alpha)I^2\sigma_Y^2/\pi$ for isotropic media $I_v = I$.

We display in figure 5 the dimensionless variance $\sigma_\eta^2/(\sigma_Y^2 II_v)$ as function of α for a few values of ϵ. For $\alpha = 0$ the variance is zero as the driving flow gradient $J = \sin\alpha$ tends to zero. The η-fluctuations reach their maximum for $\alpha = \pi/2$ since the gradient is also maximal and the condition is of pressure relief with fluctuating velocities normal to the mean free surface. If I is kept fixed while $\epsilon \to 0$, σ_η^2 also tends to zero since the values in figure 5 have to be multiplied by ϵ.

Dividing the mixed moment $C_{\varphi Y}(\mathbf{0}, 0, 0)$ by $\cos\alpha$, we can obtain the mixed moment

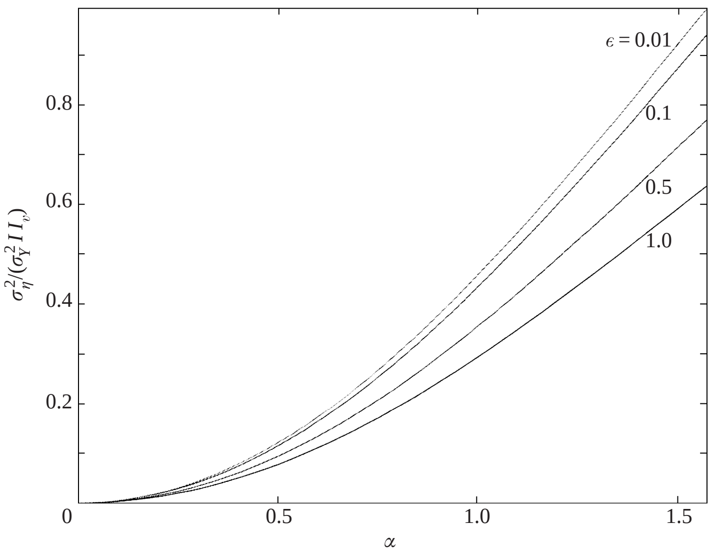

FIGURE 5. Normalized variance of the free-surface position σ_η^2, as a function of α for several values of $\epsilon = I_v/I$, the anisotropy ratio.

of η and Y at the same point (x, y) on the free surface,

$$C_{\eta Y} = -\frac{(1-\cos\alpha)I_v\sigma_Y^2}{1+\epsilon}. \tag{3.16}$$

It is seen that the correlation between Y and the free-surface position η is zero for $\alpha = 0$, i.e. for a rigid wall. This result is consistent with that pertaining to an unbounded domain, Dagan (1989). Notice that $C_{\eta Y}$ becomes negative for $\alpha > 0$ and reaches its minimal value for $\alpha = \pi/2$. The negative sign indicates that an increase of the local permeability ($Y' > 0$) causes a drop of the free surface.

Another important parameter to characterize η is the integral scale, $I_\eta = \int_0^\infty C_\eta(r_x, 0)\mathrm{d}r_x/\sigma_\eta^2$ which by (2.29) is the same as that of φ_1 on $z = 0$. By a quadrature we obtain its value,

$$I_{\eta_x} = I_{\varphi_x} = \frac{I\sin\alpha[\tanh^{-1}(\sin\alpha)](1-\epsilon^2)^{1/2}}{(1-\cos\alpha)\arctan(1-\epsilon^2/\epsilon)^{1/2}}. \tag{3.17}$$

We have represented in figure 6 the dependence of I_{η_x}/I upon α, for a few values of ϵ, showing that an increase in α leads to an increase in the integral scale.

4. Statistical moments of flux

The specific discharge $\boldsymbol{q} = (q_x, q_y, q_z)$ is given by $\boldsymbol{q} = -\mathrm{e}^Y\nabla\varphi$ such that in the first-order approximation the mean of $\boldsymbol{q}$, $\boldsymbol{q}_0$, and its first-order fluctuation $\boldsymbol{q}_1$ are given by

$$\boldsymbol{q}_0 = -K_G\begin{pmatrix} -\sin\alpha \\ 0 \\ 0 \end{pmatrix} \quad \text{and} \quad \boldsymbol{q}_1 = -K_G\begin{pmatrix} -Y'\sin\alpha + (\partial\varphi_1/\partial x) \\ \partial\varphi_1/\partial y \\ \partial\varphi_1/\partial z \end{pmatrix} \tag{4.1}$$

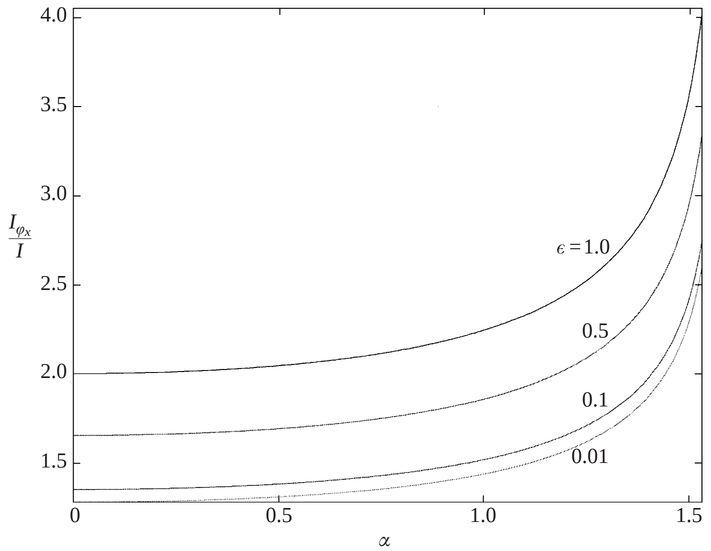

FIGURE 6. Normalized integral scale of φ_1 as a function of angle of mean incline α for several values of $\epsilon = I_v/I$, the anisotropy ratio.

respectively, where $K_G = \mathrm{e}^{m_Y}$ is the geometric mean. Multiplying $\boldsymbol{q}_1(\boldsymbol{x})$ by $\boldsymbol{q}_1(\tilde{\boldsymbol{x}})$ and averaging gives the covariances,

$$C_{q_x} = K_G^2 \left[(\sin^2 \alpha) C_Y(\boldsymbol{r}, z, \tilde{z}) - \frac{\partial^2 C_\varphi(\boldsymbol{r}, z, \tilde{z})}{\partial r_x^2} - \sin\alpha \left(\frac{\partial C_{\varphi Y}(\boldsymbol{r}, z, \tilde{z})}{\partial r_x} - \frac{\partial C_{\varphi Y}(-\boldsymbol{r}, \tilde{z}, z)}{\partial r_x} \right) \right], \tag{4.2}$$

$$C_{q_y} = K_G^2 \frac{\partial^2 C_\varphi(\boldsymbol{r}, z, \tilde{z})}{\partial r_y^2}, \tag{4.3}$$

$$C_{q_z} = K_G^2 \frac{\partial^2 C_\varphi(\boldsymbol{r}, z, \tilde{z})}{\partial z \tilde{z}}, \tag{4.4}$$

to second order in σ_Y. As we know the analytical form of C_φ and $C_{\varphi Y}$ in the Fourier space, we now express the covariance of flux in terms of the Fourier transforms of C_φ and $C_{\varphi Y}$. For example, the x-component of the flux covariance is given by

$$C_{q_x}(\boldsymbol{r}, z, \tilde{z}) = K_G^2 \left[C_Y \sin^2 \alpha + \frac{1}{2\pi} \int_{-\infty}^{\infty} \int_{-\infty}^{\infty} k_1^2 \hat{C}_\varphi(\boldsymbol{k}, z, \tilde{z}) \mathrm{e}^{-\mathrm{i} r_x k_1 - \mathrm{i} r_y k_2} \mathrm{d}k_1 \mathrm{d}k_2 + \frac{\mathrm{i} \sin\alpha}{2\pi} \int_{-\infty}^{\infty} \int_{-\infty}^{\infty} k_1 (\hat{C}_{\varphi Y}(\boldsymbol{k}, z, \tilde{z}) - \hat{C}_{\varphi Y}(-\boldsymbol{k}, \tilde{z}, z)) \mathrm{e}^{-\mathrm{i} r_x k_1 - \mathrm{i} r_y k_2} \mathrm{d}k_1 \mathrm{d}k_2 \right]. \tag{4.5}$$

Setting $r_x = r_y = 0$ and $z = \tilde{z}$ yields the variance of q_x. On the free surface, i.e. when $z = 0$, the analytic solution of $\sigma_{q_x}^2$ is given by

$$\sigma_{q_x}^2 = K_G^2 \sigma_Y^2 \left[\sin^2 \alpha + \frac{c_2 \epsilon}{4(1-\epsilon^2)} \left(\frac{\tan^{-1}(1-\epsilon^2/\epsilon^2)^{1/2}}{(1-\epsilon^2)^{1/2}} - \epsilon \right) \right], \tag{4.6}$$

where $c_2 = \cot^2\alpha[6\cos\alpha - 5 + \cos 2\alpha(1 - 2\cos\alpha)]$.

In a similar manner, we can calculate $\sigma^2_{q_y}(z)$, and $\sigma^2_{q_z}(z)$, the variance of y and z components of specific discharge respectively. This development is given in Appendix B, and it yields the following values on the free surface, $z = 0$:

$$\sigma^2_{q_y} = \frac{1}{8}K_G^2\sigma_Y^2 \cos^2(2\alpha)\sec^4\left(\frac{\alpha}{2}\right)\frac{\epsilon}{1-\epsilon^2}\left(\frac{\tan^{-1}(1-\epsilon^2/\epsilon^2)^{1/2}}{(1-\epsilon^2)^{1/2}} - \epsilon\right), \qquad (4.7)$$

$$\sigma^2_{q_z} = 2K_G^2\sigma_Y^2(1 + 2\cos\alpha)\sin^4\left(\frac{\alpha}{2}\right)\frac{\epsilon}{1-\epsilon^2}\left(\frac{\tan^{-1}(1-\epsilon^2/\epsilon^2)^{1/2}}{(1-\epsilon^2)^{1/2}} - \epsilon\right). \qquad (4.8)$$

In an isotropic medium we find that the specific discharge variances are given by

$$\sigma^2_{q_x} = K_G^2\sigma_Y^2[\sin^2\alpha + c_2/6], \quad \sigma^2_{q_y} = K_G^2\sigma_Y^2\cos^2(2\alpha)\sec^4(\alpha/2)/12,$$

$$\sigma^2_{q_z} = 4K_G^2\sigma_Y^2(1 + 2\cos\alpha)\sin^4(\alpha/2)/3.$$

Away from the free surface, the specific discharge variance can be computed numerically via one numerical quadrature (see Appendix B) and can be computed analytically at $z = -\infty$. At $z = -\infty$, the problem is identical to the problem of mean uniform flow in an infinite medium such that in an isotropic medium, $\sigma^2_{q_x} = 8\sigma_Y^2 e^{2m_Y}\sin^2\alpha/15$ and $\sigma^2_{q_x} = \sigma_Y^2 e^{2m_Y}\sin^2\alpha/15$ (e.g. Dagan 1989).

The longitudinal integral scale of specific discharge in the direction of mean uniform flow is given by

$$I_{q_x}(z) = \frac{\int_0^\infty C_{q_x}(r_x, 0, z, z)\mathrm{d}r_x}{\sigma^2_{q_x}(z)}. \qquad (4.9)$$

Integrating in terms of r_x in (4.5), utilizing the fact that $\int_0^\infty e^{-ir_xk_1}\mathrm{d}r_x = \pi\delta(k_1)$, and then evaluating the integral in k_1 yields

$$I_{q_x}(z) = \frac{15}{8}\frac{\sigma^2_{q_x}(-\infty)}{\sigma^2_{q_x}(z)}I, \qquad (4.10)$$

i.e. $\sigma^2_{q_x}(z)I_{q_x}(z) = \sigma_Y^2K_G^2\sin^2\alpha I$.

In figures 7 and 8 we present the normalized x- and z-direction flux variances respectively in an isotropic medium for $\alpha = \pi/36, \pi/6, \pi/4$, and $\pi/2$. The flux variance is normalized by its value at infinity and we notice a rapid convergence of the flux to its value at infinity, within 3 to 4 vertical length scales, I_v, away from the free surface. On and near the free surface, we notice that the angle of mean incline acts to increase the relative flux variances, which reach their maximal values at $\alpha = \pi/2$, and their minimal values as α approaches zero. Regardless of α, we see in figure 7 that, the variance of q_x is at its maximum on the free surface, and quickly reduces to its infinite-medium value. In contrast, it is seen in figure 8 that for very small α, the variance of the z-direction flux is at its minimum on the free surface, and then increases to its infinite-medium solution, whereas for larger angles the variance is maximal on the free surface. This is understandable in the light of the rigid wall and pressure release analogies to the free-surface boundary condition at $\alpha = 0$ and $\alpha = \pi/2$ respectively.

Examining the behaviour of the integral scale I_{q_x} in (4.10), it is seen that I_{q_x}

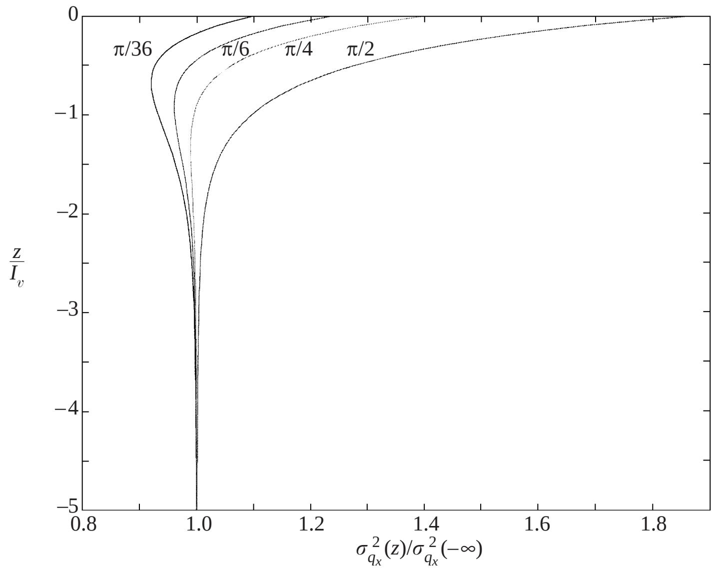

FIGURE 7. Normalized variance of x-direction flux, $\sigma^2_{q_x}/\sigma^2_{q_x}(-\infty)$, as a function of dimensionless depth z/I_v for several angles of mean incline α.

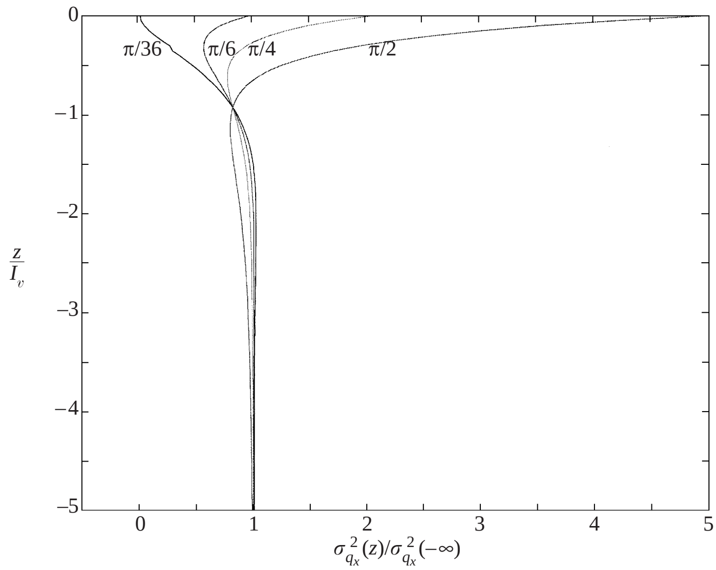

FIGURE 8. Normalized variance of z-direction flux, $\sigma^2_{q_z}/\sigma^2_{q_z}(-\infty)$, as a function of dimensionless depth z/I_v for several angles of mean incline α.

is inversely proportional to the normalized flux. The results for the normalized x-direction flux q_x in figure 7 therefore show us that the integral scale I_{q_x} holds its minimal value on the free surface, and rapidly increases to its infinite medium value. In contrast, the product $\sigma^2_{q_x} I_{q_x}$, of interest in transport, is constant and equal to its value in an unbounded domain.

5. Summary and conclusions

We have derived the statistical moments of flow variables in the presence of a free surface in a randomly heterogeneous medium in which the mean flow is uniform. Making the assumption of mild heterogeneity in the hydraulic conductivity, we have used a perturbation expansion approach to derive an analytical solution for the free-surface position mean and variance. Additionally, we were able to compute the mean and variance of pressure head and fluid flux analytically on the free surface and numerically beneath it. The impact of the angle of mean incline on the statistical moments of pressure head and flux field was examined.

The variance and integral scale of the free-surface fluctuations are of interest in many applications in which the flow is uniform or slowly varying. They are indicative of the departure from the mean of observed water table elevations in aquifers. In the case of interface flows, the standard deviation can be regarded as a measure of heterogeneity-induced mixing. It is seen that both variance and integral scales are minimal at small slopes and increase with α.

Another interesting result is the slow convergence with depth of the head variance from its free-surface value to that pertaining to an unbounded domain. In fact, the influence of the free-surface boundary on head fluctuations is felt beyond a distance of ten integral scales. The flux and the associated velocity behaviour is different: the influence of the free surface is felt in a boundary layer. At a depth of approximately three integral scales, the flux components variance reaches its value in an unbounded domain.

The analytical and qualitative results of this work can be applied to all free-surface problems in which the mean flow is slowly varying. Important examples include free-surface flow towards a well sufficiently far away from it and interface flow towards the sea far from the outlet.

This research was supported by a grant from the Ministry of Science, Israel.

Appendix A. Derivation of the solution of the head

As our problem is stationary in the (x, y)-plane, we perform a change of variables to transform (3.1)–(3.4) to the most relevant coordinate system, $r_x = x - \tilde{x}$ and $r_y = y - \tilde{y}$:

$$\Delta C_{\varphi} - \sin\alpha \frac{\partial C_{\varphi Y}(-\boldsymbol{r}, \tilde{z}, z)}{\partial r_x} = 0 \quad (z \leqslant 0), \qquad \text{(A 1)}$$

$$\frac{\partial C_{\varphi}}{\partial z} + \tan\alpha \frac{\partial C_{\varphi}}{\partial r_x} = 0 \quad (z = 0), \qquad \text{(A 2)}$$

$$\Delta C_{\varphi Y} - \sin\alpha \frac{\partial C_Y(\boldsymbol{r}, z, \tilde{z})}{\partial r_x} = 0 \quad (z \leqslant 0), \qquad \text{(A 3)}$$

$$\frac{\partial C_{\varphi Y}}{\partial z} + \tan\alpha \frac{\partial C_{\varphi Y}}{\partial r_x} = 0 \quad (z = 0), \qquad \text{(A 4)}$$

where the Laplacian is in terms of $(\boldsymbol{r}, z)$, $C_{\varphi} = C_{\varphi}(\boldsymbol{r}, z, \tilde{z})$, and $C_{\varphi Y} = C_{\varphi Y}(\boldsymbol{r}, z, \tilde{z}) = C_{\varphi Y}(\boldsymbol{x}, \tilde{\boldsymbol{x}})$. Notice that the $C_{\varphi Y}(\tilde{\boldsymbol{x}}, \boldsymbol{x})$ of (3.3) was replaced by $C_{\varphi Y}(-\boldsymbol{r}, \tilde{z}, z)$ as the change of order between $\boldsymbol{x}$ and $\tilde{\boldsymbol{x}}$ involves a change in the order between z and $\tilde{z}$ as well as a change of sign in r_x and r_y. Taking the Fourier transform of these equations results in

$$(\hat{C}_\varphi)_{zz} - \kappa^2\hat{C}_\varphi + \mathrm{i}k_1 \sin\alpha \hat{C}_{\varphi Y}(-\boldsymbol{k}, \tilde{z}, z) = 0 \quad (z \leqslant 0), \tag{A 5}$$

$$(\hat{C}_\varphi)_z - \mathrm{i}k_1 \tan\alpha \hat{C}_\varphi = 0 \quad (z = 0), \tag{A 6}$$

$$(\hat{C}_{\varphi Y})_{zz} - \kappa^2\hat{C}_{\varphi Y} + \mathrm{i}k_1 \sin\alpha \hat{C}_Y(\boldsymbol{k}, z, \tilde{z}) = 0 \quad (z \leqslant 0), \tag{A 7}$$

$$(\hat{C}_{\varphi Y})_z - \mathrm{i}k_1 \tan\alpha \hat{C}_{\varphi Y} = 0 \quad (z = 0), \tag{A 8}$$

whose solution is given in terms of the Green's function $G(z, \xi, \boldsymbol{k})$ via (3.5)–(3.6). Using the Green's function (3.9) we calculate $\hat{C}_{\varphi Y}(\boldsymbol{k}, z, z)$ according to (3.5) to obtain

$$\hat{C}_{\varphi Y}(\boldsymbol{k}, z, z) = \frac{\mathrm{i}k_1 I_v I^2 \sigma_Y^2 \sin\alpha}{\pi\kappa} \exp\left(\frac{-(I^2 - I_v^2)\kappa^2}{\pi}\right) \left[2\mathrm{erfc}\left(\frac{\kappa I_v}{\pi^{1/2}}\right) - \mathrm{erfc}\left(\frac{2\kappa I_v^2 - \pi z}{2I_v \pi^{1/2}}\right) + \frac{(\kappa + \mathrm{i}bk_1)^2}{\kappa^2 + b^2k_1^2} \mathrm{e}^{2\kappa z} \mathrm{erfc}\left(\frac{2\kappa I_v^2 + \pi z}{2I_v \pi^{1/2}}\right)\right]. \tag{A 9}$$

Similarly, we can obtain an analytic expression for $\hat{C}_\varphi$.

$$\begin{aligned}\hat{C}_\varphi(\boldsymbol{k}, z, z) = {} & \frac{k_1^2 I_v I^2 \sigma_Y^2 \sin^2\alpha}{\pi^2\kappa^5(\kappa^2 + b^2k_1^2)} \exp\left(\frac{-(I^2 - I_v^2)\kappa^2}{\pi}\right) \\ & \times \left[2I_v\kappa^3 \exp\left(-\frac{\kappa^2 I_v^2}{\pi}\right)\left(-2b^2k_1^2 \exp\left(\kappa z - \frac{\pi z^2}{4I_v^2}\right)\right.\right. \\ & \left. + \mathrm{e}^{2kz}(-\kappa^2 + b^2k_1^2) + \kappa^2 + b^2k_1^2\right) + (2(\mathrm{e}^{2kz} - 1)\kappa^4 I_v^2 \\ & + (b^2k_1^2\pi + \kappa^2(\pi - 2b^2k_1^2I_v^2))(1 + \mathrm{e}^{2\kappa z}))\mathrm{erfc}\left(\frac{\kappa I_v}{\pi^{1/2}}\right) \\ & + (\kappa^3(2\kappa I_v^2 - \pi z) + b^2k_1^2(2\kappa^2 I_v^2 - \pi - \kappa\pi z)) \\ & \times \mathrm{erfc}\left(\frac{2\kappa I_v^2 - \pi z}{2I_v\pi^{1/2}}\right) + \mathrm{e}^{2\kappa z}(-\kappa^3(2\kappa I_v^2 + \pi z) \\ & \left. + b^2k_1^2(2\kappa^2 I_v^2 - \pi + \kappa\pi z))\mathrm{erfc}\left(\frac{2\kappa I_v^2 + \pi z}{2I_v\pi^{1/2}}\right)\right],\end{aligned} \tag{A 10}$$

where $b = \tan\alpha$.

Appendix B. Derivation of the velocity covariance

In order to obtain the y and z components of the velocity covariance shown in (4.3) and (4.4) we first represent the covariance of φ_1 in terms of its Fourier transform in polar coordinates (s, θ) such that

$$C_{q_y}(\boldsymbol{r}, z, \tilde{z}) = -K_G^2 \frac{1}{2\pi} \int_0^\infty \int_0^{2\pi} \hat{C}_\varphi(\boldsymbol{k}, z, \tilde{z}) s^3 \sin^2\theta \mathrm{e}^{-\mathrm{i}r_x s\cos\theta - \mathrm{i}r_y s\sin\theta} \mathrm{d}\theta \mathrm{d}s, \tag{B 1}$$

$$C_{q_z}(\boldsymbol{r}, z, \tilde{z}) = K_G^2 \frac{1}{2\pi} \int_0^\infty \int_0^{2\pi} \frac{\partial^2 \hat{C}_\varphi(\boldsymbol{k}, z, \tilde{z})}{\partial z \partial\tilde{z}} \mathrm{e}^{-\mathrm{i}r_x s\cos\theta - \mathrm{i}r_y s\sin\theta} s \mathrm{d}\theta \mathrm{d}s, \tag{B 2}$$

where $\boldsymbol{k} = (s\cos\theta, s\sin\theta)$. To compute the variance on the free surface, we take $r_x = 0$, $r_y = 0$, differentiate $\hat{C}_\varphi(s, \theta, z, \tilde{z})$ with respect to z and $\tilde{z}$, in (B 2), and take the limit as $z \to 0$ and $\tilde{z} \to 0$ yielding (4.7) and (4.8).

For $z<0$, we can semi-analytically calculate $\sigma_q^2(z)$. Considering the solutions for $\hat{C}_{\varphi Y}(\boldsymbol{k},z,z)$ and $\hat{C}_{\varphi}(\boldsymbol{k},z,z)$ shown in (A 9)–(A 10), we can analytically compute one of two necessary quadratures by setting $r_x=r_y=0$, $\tilde{z}=z$, and changing to polar coordinates in (4.5). This transforms the expression for the x-direction velocity variance to

$$\sigma_{q_x}^2(z)=\mathrm{e}^{2m_Y}\left[\sigma_Y^2\sin^2\alpha+\frac{1}{2\pi}\int_0^{\infty}\int_0^{2\pi}\hat{C}_{\varphi}(\boldsymbol{k},z,z)s^3\cos^2\theta\,\mathrm{d}\theta\,\mathrm{d}s\right.$$
$$\left.+\frac{\mathrm{i}\sin\alpha}{2\pi}\int_0^{\infty}\int_0^{2\pi}(\hat{C}_{\varphi Y}(\boldsymbol{k},z,z)-\hat{C}_{\varphi Y}(-\boldsymbol{k},z,z))s^2\cos\theta\,\mathrm{d}\theta\,\mathrm{d}s\right]. \quad \text{(B 3)}$$

Considering (A 9)–(A 10) we can analytically calculate the integral in θ yielding

$$\sigma_{q_x}^2(z)=a^2\sigma_Y^2\mathrm{e}^{2m_Y}\left(1+\frac{I_vI^2}{8\pi^2b^4c}\int_0^{\infty}s^2\exp\left(\frac{-(I^2-I_v^2)s^2}{\pi}\right)\right.$$
$$\times\left(2\exp\left(\frac{I_v^2s^2}{\pi}\right)\left(-2(-8(8-4b^2+3b^4)c)\exp\left(sz-\frac{\pi z^2}{4I_v^2}\right)\right.\right.$$
$$\left.+(3b^4c+(-16+(16-8b^2+3b^4)c)\mathrm{e}^{2sz})\right)I_vs+(-b^4c(13\pi+6I_v^2s^2)$$
$$+\mathrm{e}^{2sz}(3b^4c\pi-2(-16+(16-8b^2+3b^4)c)I_v^2s^2))\mathrm{erfc}\left[\frac{I_vs}{\pi^{1/2}}\right]$$
$$+(6b^4cI_v^2s^2+\pi(8+c(-8+4b^2+b^4(5-3sz))))\mathrm{erfc}\left[\frac{2I_v^2s-\pi z}{2I_v\pi^{1/2}}\right]$$
$$+\mathrm{e}^{2z}(2(-16+(16-8b^2+3b^4)c)I_v^2s^2+\pi(8(-1+c)(-1+2sz)$$
$$\left.\left.+b^4c(5+3sz)-4b^2(-8+7c+2csz)))\mathrm{erfc}\left[\frac{2I_v^2s+\pi z}{2I_v\pi^{1/2}}\right]\right)\right)\mathrm{d}s, \quad \text{(B 4)}$$

where $a=\sin\alpha$, $b=\tan\alpha$ and $c=(1+b^2)^{1/2}=\sec\alpha$.

In order to calculate $\sigma_{q_z}^2(z)$, we must first evaluate the derivatives in z and $\tilde{z}$, and then take the limit as $\tilde{z}\to z$. Performing these operations and integrating in θ yields

$$\sigma_{q_z}^2(z)=\frac{1}{2\pi}\int_0^{\infty}\frac{1}{b^2c\pi}a^2I_vh^2\sigma_Y^2\left(2\exp\left(-\left(\frac{I_vh^2s^2}{\pi}-\frac{\pi z^2}{4I_v^2}\right)\right)\right.$$
$$\times\left(4(-1+c)\mathrm{e}^{sz}-b^2c\exp\left(\frac{\pi z^2}{4I_v^2}\right)+(4-4c+b^2c)\exp\left(2sz+\frac{\pi z^2}{4I_v^2}\right)\right)I_v^2s^3$$
$$+\exp\left(\frac{-(I_vh^2-I_v^2)s^2}{\pi}\right)I_vs^2(-8\mathrm{e}^{2sz}I_v^2s^2+c(b^2\pi+2b^2I_v^2s^2$$
$$+\mathrm{e}^{2sz}(b^2\pi-2(-4+b^2)I_v^2s^2)))\mathrm{erfc}\left[\frac{I_vs}{(\pi)^{1/2}}\right]+\exp\left(\frac{-(I_vh^2-I_v^2)s^2}{\pi}\right)$$
$$\times I_vs^2(2\pi+c(-2\pi-2b^2I_v^2s^2+b^2\pi sz))\mathrm{erfc}\left[\frac{2I_v^2s-\pi z}{2I_v\pi^{1/2}}\right]$$
$$+\exp\left(\frac{-(I_vh^2-I_v^2)s^2}{\pi}+2sz\right)I_vs^2(2\pi+8I_v^2s^2+4\pi sz$$
$$\left.+c(-2\pi+2(-4+b^2)I_v^2s^2+(-4+b^2)\pi sz))\mathrm{erfc}\left[\frac{2I_v^2s+\pi z}{2I_v(\pi)^{1/2}}\right]\right)\mathrm{d}s.$$

REFERENCES

Bear, J. 1972 *Dynamics of Fluids in Porous Media*. Elsevier.

Dagan, G. 1984 Solute transport in heterogeneous porous formations. *J. Fluid Mech.* **145**, 151–177.

Dagan, G. 1989 *Flow and Transport in Porous Formations*. Springer.

Dagan, G. & Zeitoun, D. 1998 Free-surface flow toward a well and interface upconing in stratified aquifers of random conductivity. *Water Resour. Res.* **34**, 3191–3196.

Fenton, G. & Griffiths, D. 1996 Statistics of free surface flow through a stochastic earth dam. *J. Geotech. Engng, ASCE* **122**, 427–436.

Lessoff, S., Indelman, P. & Dagan, G. 2000 A note on the influence of a constant velocity boundary condition on flow and transport in heterogeneous formations. *Water Resour. Res.* **36**, 3095–3101.

Paleologos, E., Neuman, S. & Tartakovsky, D. 1996 Effective hydraulic conductivity of bounded, strongly heterogeneous porous media. *Water Resour. Res.* **32**, 1333–1341.

Polubarinova-Kotchina, P. Y. 1962 *Theory of Groundwater Movement*. Princeton University Press (translation from Russian).

Rubin, Y. & Dagan, G. 1988 Stochastic analysis of boundaries effects on head spatial variability in heterogeneous aquifers, 1. constant head boundaries. *Water Resour. Res.* **24**, 1689–1697.

Rubin, Y. & Dagan, G. 1989 Stochastic analysis of boundaries effects on head spatial variability in heterogeneous aquifers, 2. impervious boundary. *Water Resour. Res.* **25**, 707–712.

Tartakovsky, D. 1999 Stochastic modeling of heterogeneous phreatic aquifers. *Water Resour. Res.* **35**, 3941–3945.

Tartakovsky, D. & Winter, C. 2001 Dynamics of free surfaces in random porous media. *SIAM J. Appl. Maths* **61**, 1857–1876.